an intimate mechanism is that k_2 will also include k_{-a}, which must be sensitive to the basicity of the entering amine since this process involves the breaking of the Pt–N bond. This is also found in the reactions of the sulfoxide system, where α = 0.41 and 0.58 for the bis(dimethyl sulfoxide) and the -pse complexes, respectively. On going to the thioether analogues, the absence of the large differences between the labilities of a bis monodentate and a chelate system suggests that the bond-breaking part of the intimate mechanism is less important and that the system has moved in the direction where $k_d > k_{-a}$ and $k_2 = k_a$. This would require that k_2 was not sensitive to differences in the bond-breaking rate constants and also far less sensitive to amine basicity (smaller α). This is indeed what has been observed (α = 0.18 and 0.14 for the bis(dimethyl sulfide) and -pte complexes, respectively).

Acknowledgment. We thank Professor P. Uguagliati for some kinetic computing, Miss S. Boesso and Mrs. L. Gemelli for technical assistance, and the Italian Council for Research, CNR, Rome, for financial support in a bilateral project.

Registry No. *trans*-$[Pt(Me_2S)_2Cl_2]$, 17457-51-1; *cis*-$[Pt(Me_2S)_2Cl_2]$, 17836-09-8; 4-methylpyridine, 108-89-4; pyridine, 110-86-1; 4-cyanopyridine, 100-48-1; pyrimidine, 289-95-2; pyrazine, 290-37-9; 3,4-dimethylpyridine, 583-58-4; 3,5-dimethylpyridine, 591-22-0; 3-methylpyridine, 108-99-6; 2,4-dimethylpyridine, 108-47-4; 2-methylpyridine, 109-06-8.

Supplementary Material Available: Listings of first-order rate constants (3 pages). Ordering information is given on any current masthead page.

Contribution from the Department of Chemistry, Tulane University, New Orleans, Louisiana 70118

Kinetic Studies of Ligand Substitution Reactions and General-Base Catalysis in Amine-Ligand Exchange Processes for Group 6B Metal Carbonyl Amine Derivatives. Kinetic and Spectroscopic Evidence for Hydrogen-Bonded Intermediates

DONALD J. DARENSBOURG* and JOHN A. EWEN

Received April 16, 1981

The decomposition and ligand substitution reactions of group 6B metal pentacarbonyl piperidine derivatives with phosphines have been studied. The reactions are catalyzed by the Lewis bases $OP(n\text{-}C_4H_9)_3$ and tetrahydrofuran (THF). It is concluded that the results are best accounted for in terms of hydrogen-bonded intermediates in the general-base catalysis with the mechanism for catalysis being closely analogous to a dissociative interchange (I_d) pathway. The intermediates have been observed and characterized by infrared spectroscopy.

Introduction

The kinetics of amine substitution reactions for group 6B metal pentacarbonyl amine derivatives with phosphorus donor ligands (eq 1) have been shown to obey the empirical rate law

$$M(CO)_5(\text{amine}) + PR_3 \rightarrow M(CO)_5PR_3 + \text{amine} \quad (1)$$

given by eq 2.[1-4] This corresponds to the rate constant expression in eq 3 upon integration.

$$\text{rate} = (k_1 + k_2[PR_3])[M(CO)_5(\text{amine})] \quad (2)$$

$$k_{obsd} = k_1 + k_2[PR_3] \quad (3)$$

It is generally accepted that the first-order term (k_1 in eq 2) represents a purely dissociative (D) mechanism. The proposed dissociative (D) mechanism giving rise to k_1 is given by eq 4 and 5. The rate constant expression is given by eq 6, which reduces to $k_{obsd} = k_1$ for the condition that is usually satisfied, $k_{-1}[A] \ll k_0[B]$.[5]

$$M(L)_nA \underset{k_{-1}}{\overset{k_1}{\rightleftharpoons}} M(L)_n + A \quad (4)$$

$$M(L)_n + B \xrightarrow[\text{rapid}]{k_0} M(L)_nB \quad (5)$$

$$k_{obsd} = \frac{k_1k_0[B]}{k_{-1}[A] + k_0[B]} \quad (6)$$

Mechanisms that have been postulated to accommodate the rate data presume a concurrent bimolecular pathway (k_2 in eq 2), which could involve either attack by PR_3 (at the metal center or at a carbonyl carbon atom) resulting in displacement of the amine ligand to form $M(CO)_5PR_3$ or a rapid associative–dissociative equilibrium occurring by an unknown process followed by a rate-determining dissociative step.[4] This latter mechanism (a dissociative interchange or I_d substitution pathway[6]) proceeding to completion (eq 7–10) obeys the rate constant expressions provided in eq 11 and 12. If $K_2[A] \ll$

$$M(L)_nA + B \overset{K_1}{\rightleftharpoons} M(L)_nA\cdot B \quad (7)$$

$$M(L)_nA\cdot B \xrightarrow{k'_2} M(L)_nB\cdot A \quad (8)$$

$$M(L)_nB\cdot A \xrightarrow{\text{fast}} M(L)_nB + A \quad (9)$$

$$M(L)_nA + A \overset{K_2}{\rightleftharpoons} M(L)_nA\cdot A \quad (10)$$

$$k_{obsd} = \frac{k'_2K_1[B]}{1 + K_1[B] + K_2[A]} \quad (11)$$

$$\frac{1}{k_{obsd}} = \frac{1}{k'_2} + \frac{1 + K_2[A]}{k'_2K_1[B]} \quad (12)$$

(1) Darensbourg, D. J.; Brown, T. L. *Inorg. Chem.* **1968**, *7*, 1679.
(2) Ingemason, C. M.; Angelici, R. J. *Inorg. Chem.* **1968**, *7*, 2646.
(3) Dennenberg, R. J.; Darensbourg, D. J. *Inorg. Chem.* **1972**, *11*, 72.
(4) Covey, W. D.; Brown, T. L. *Inorg. Chem.* **1973**, *12*, 1973.
(5) Reactions are carried out generally under conditions where the concentration of the incoming ligand (B) exceeds that of the leaving ligand (A). Values of the rate constants k_{-1} and k_0 are expected to be of comparable magnitude; for an example, see ref 4.
(6) Langford, C. H.; Gray, H. B. "Ligand Substitution Processes"; W. A. Benjamin: New York, 1965.

0020-1669/81/1320-4168$01.25/0

1, $k_{obsd} = k'_2K_1[B]/(1 + K_1[B])$. Hence for concurrent I_d and D mechanisms with negligible concentrations of departing ligand A, the complete rate constant expression is given by eq 13. This reduces to the expression in eq 14 providing $K_1[B]$

$$k_{obsd} = k_1 + \frac{k'_2K_1[B]}{1 + K_1[B]} \tag{13}$$

$\ll 1$. Equation 14 is mathematically equivalent to the empirical rate constant expression (eq 3).

$$k_{obsd} = k_1 + k'_2K_1[B] \tag{14}$$

The experimentally determined k_1 and k_2 values (eq 3) are thus felt to arise from dissociative mechanisms and are anticipated to exhibit similar trends since the bimolecular pathway arises only as a consequence of the incoming ligand replacing a solvent molecule in the complex's second coordination sphere.

In an earlier preliminary communication,[7] we presented kinetic and spectroscopic evidence for the formation of a kinetically labile hydrogen-bonded adduct during the reaction of $Mo(CO)_5NHC_5H_{10}$ with $P(C_6H_5)_3$ in the presence of (n-$C_4H_9)_3P{=}O$ (eq 15–18), where C represents the (n-

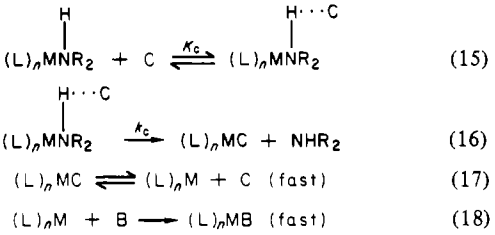

$C_4H_9)_3P{=}O$ catalyst, B the incoming $P(C_6H_5)_3$, and NHR_2 the departing piperidine ligand. Alternatively, B may directly add to the $(L)_nM$ intermediate as C removes the amine from the metal center. However, the rapid reversible association process (eq 15) increases the effective concentration or activity of C at the reaction site and hence serves as an "entropy trap". In any case this would not affect the kinetic analysis provided here. The rate constant expressions for the general-base-catalyzed path are given by eq 19 and 20 providing that the rate of formation of the intermediate $(L)_nMC$ is very much slower than that of its subsequent reaction with B.

$$k_{obsd} = \frac{k_cK_c[C]}{1 + K_c[C]} \tag{19}$$

$$\frac{1}{k_{obsd}} = \frac{1}{k_c} + \frac{1}{k_cK_c[C]} \tag{20}$$

For the D, I_d, and general-base-catalyzed (I_{bc}) pathways, all operating concurrently with kinetically negligible concentrations of both A and $M(L)_nC$ (Scheme I), the rate constant expression is given by eq 21. Equation 21 cannot be cast into

$$k_{obsd} = \frac{k_1 + k'_2K_1[B] + k_cK_c[C]}{1 + K_1[B] + K_c[C]} \tag{21}$$

an analytically convenient inverted linear form; however, eq 20 can be used as a valid approximation under conditions where $(k_1 + k'_2K_1[B]) \ll k_cK_c[C]$ and $K_1[B] \ll 1$.

The present study is concerned with a more extensive investigation of the mechanism of the general-base-catalyzed pathway involving hydrogen-bonded intermediates. We have also attempted to identify reasonable causes for the inconsistencies reported for both k_1 and k_2 (eq 3).[1-4] In addition particularly simple explanations are suggested to account for the solvent effects on the rates and mechanisms of ligand substitution processes of these species, for the solvent effects on the visible spectra and the ν(CO) infrared spectra of these metal carbonyl amine derivatives, and finally for the observation of a second-order photochemical substitution reaction between $Mo(CO)_5NHC_5H_{10}$ and $P(C_6H_5)_3$ in hexane.

Scheme I

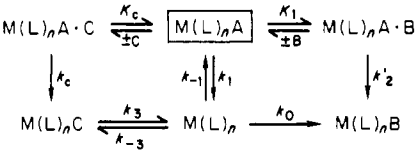

Experimental Section

A. Materials. $Cr(CO)_6$ was purchased from Strem Chemicals. $Mo(CO)_6$ and $W(CO)_6$ were gifts from Climax Molybdenum Co. Tri-n-butylphosphine oxide was donated by Arapahoe Chemicals. The liquid phosphines, phosphites, and phosphates used were obtained from Aldrich Chemical Co. and were purified by fractional vacuum distillation prior to use and stored under nitrogen. Liquid amines were stored over NaOH pellets and distilled under reduced pressure from barium oxide when required. Hexamethylenephosphoric triamide (HMPA) was distilled over BaO and dried over CaH_2. Tri-n-butylphosphine oxide was dried by heating under vacuum prior to use. Triphenylphosphine was purified by recrystallization from a $CHCl_3$/MeOH mixture. Spectral grade solvents were used without further purification. Tetrahydrofuran (THF) was distilled from sodium/benzophenone immediately before use. All preparations and kinetic runs were carried out under an inert atmosphere of N_2 or Ar and were protected from light unless noted otherwise. The solvents were degassed with three freeze–thaw cycles. Photochemical syntheses were performed in quartz vessels, and thermal preparations were heated by means of an oil bath and stirred magnetically.

B. Instrumentation. Melting points were measured in open capillary tubes with a Thomas-Hoover apparatus, and the uncorrected values compared well with those reported in the literature. Visible spectra were obtained with use of a Cary 14 spectrophotometer with matched 1.0-cm quartz cells. Infrared spectra were measured on a Perkin-Elmer 521 spectrophotometer equipped with a linear absorbance potentiometer. The absorbance spectra for Beer's law plots were recorded on an expanded scale with use of matched sodium chloride cells whose path lengths were determined by the interference fringe method. The infrared spectra were calibrated against water vapor and gaseous CO spectra below and above 2000 cm^{-1}, respectively. The CO gas was contained in a 10-cm cell at approximately 0.5 atm.

C. Preparation of Complexes. M(CO)$_5$(amine) for M = Cr, Mo, W and Amine = Pyridine, Piperidine, Cyclohexylamine, Morpholine. Equimolar amounts of piperidine and $Mo(CO)_6$ were reacted in refluxing heptane for 1.5 h. The solvent was evaporated under reduced pressure at room temperature. Residual unreacted $Mo(CO)_6$ was removed by vacuum sublimation at 45 °C, and the yellow product was purified by recrystallization from hexane at −80 °C and found to contain no detectable $Mo(CO)_6$ by infrared analysis. Pyridine, cyclohexylamine, and morpholine complexes were prepared similarly. Chromium and tungsten pentacarbonyl amine derivatives were synthesized and purified with use of the same procedures or with an excess of the hexacarbonyl. Attempts to prepare the tertiary amine derivative $Mo(CO)_5N(n\text{-}C_4H_9)_3$ failed, presumably due to the thermal instability of the product.

More satisfactory yields of the piperidine derivatives were obtained with use of a photochemical method. In a typical preparation 9 mmol of $Cr(CO)_6$ and a 10-fold excess of piperidine in 50 mL of THF were irradiated with a 550-W Hanovia mercury lamp positioned 18 in. from a 100-mL flask. The reaction vessel was equipped with a side arm sealed with a rubber septum and was fitted with a condenser. The apparatus was surrounded by an aluminum foil reflector. Samples were removed with a syringe periodically and monitored by infrared analysis to determine the time of maximum yield (~4 h). Product workup and purification were as described above.

M(CO)$_5$NH$_3$ for M = Cr, Mo. The previously described procedure for preparing $Cr(CO)_5NH_3$ was employed.[8,9] The hexacarbonyls were

(7) Ewen, J.; Darensbourg, D. J. *J. Am. Chem. Soc.* **1975**, *97*, 6874.

(8) Behrens, H.; Klek, W. *Z. Anorg. Allg. Chem.* **1957**, *291*, 151.

(9) Behrens, H.; Weber, R. *Z. Anorg. Allg. Chem.* **1957**, *291*, 122.

reduced with sodium in liquid ammonia at −33 °C to $[M(CO)_5]^{2-}$ species. The dianions were oxidized to $M(CO)_5NH_3$ and H_2 with use of an aqueous solution of NH_4Cl. The product was purified by cold water washing and vacuum sublimation. Poor yields of products were obtained.

$M(CO)_5P(C_6H_5)_3$ for M = Cr, Mo, W. The triphenylphosphine derivatives were prepared in THF from the metal hexacarbonyls and triphenylphosphine by the previously described photochemical procedure. The products were purified by recrystallization from a CH_3Cl/MeOH mixture.

$M(CO)_5P(n\text{-}C_4H_9)_3$ for M = Cr, Mo, W. $M(CO)_5py$ was reacted with an excess of tri-*n*-butylphosphine at 40 °C in hexane while protecting the reaction mixture from light. An infrared spectrum of the resultant solution revealed the presence of ~100% $M(CO)_5P(n\text{-}C_4H_9)_3$. Attempts to recover a pure sample of the product by vacuum distillation of the solvent and excess tri-*n*-butylphosphine were unsuccessful.

***N*-Deuteriopiperidine.** NDC_5H_{10} was prepared according to the procedure described by Normant and co-workers via the $LiNC_5H_{10}$ salt using hexamethylenephosphoric triamide (HMPA), lithium wire, and D_2O.[10,11]

D. Kinetic Measurements. The decomposition and ligand substitution reactions of group 6B $M(CO)_5$(amine) (M = Cr, Mo, W) complexes were monitored by observing the decrease in the most intense CO stretching vibration of the starting complex or of the outer-sphere complex intermediates with time. The metal complex concentrations were generally between 10^{-3} and 10^{-4} M. The spectra were obtained with use of 1.00- and 0.10-mm matched sodium chloride cells for kinetic runs in hexane and THF, respectively. A 1.00-mm sample cell was fitted with a Beckman water jacket and used to study some reactions of $Mo(CO)_5NHC_5H_{10}$. The cell temperature was maintained to ±0.1 °C with use of a constant-temperature bath circulating water through the cell jacket. Temperatures were monitored with an accurate thermometer (±0.1 °C) as the water exited the cell. Most kinetic samples were contained in 50-mL Erlenmeyer flasks sealed with a rubber septum. These were immersed directly in the constant-temperature bath and protected from light with aluminum foil. Samples were taken by syringe techniques. Rate constants were determined under first-order or pseudo-first-order conditions with excess base with use of the linear least-squares computer program KINDAT for calculating first-order rate constants.[12] The program was used to eliminate deviant points, reject data points beyond 95% reaction completion, and adjust uncertain infinity points to obtain the best least-squares fit for the rates of product appearance.

E. Spectrophotometric Determinations of K_c for Group 6B $M(CO)_5(NHC_5H_{10})$·C Complexes with C = $(n\text{-}C_4H_9)_3P{=}O$. K_c values for hydrogen-bonded $M(CO)_5(NHC_5H_{10})$·C species were determined spectrophotometrically from changes in the infrared spectra in the ν(CO) region at 23 °C with use of the same solutions and equipment as those described for the kinetics and the computer program described by Rammette.[13] If solution absorbances at zero time were unavailable, they were obtained by extrapolation with a least-squares program of the kinetic plots.

F. Infrared Spectra in the ν(NH) Region for $M(CO)_5(NHC_5H_{10})$ Species and for Their Hydrogen-Bonded Adducts in the Presence of Lewis Bases. Frequency shifts of ν(NH) in $M(CO)_5(NHC_5H_{10})$ species were recorded in tetrachloroethylene solvent in 1.0-mm NaCl solution cells. The solutions were generally 0.1–0.5 M in complex with an excess of base ranging approximately 0.5–3.0 M for formation of the hydrogen-bonded adducts.

G. Vibrational Calculations for $M(CO)_5$(amine) Derivatives. Force constant calculations for only ^{12}CO frequency data for C_{4v} $M(CO)_5L$ species and their hydrogen-bonded adducts were performed with use of the Cotton–Kraihanzel method.[14]

Results

A. Infrared and Visible Spectra of $M(CO)_5$(amine) Derivatives and Their Hydrogen-Bonded Adducts. Upon addition of the Lewis bases listed in Table I to solutions of $M(CO)(NHC_5H_{10})$ (M = Cr, Mo, W) or to $Cr(CO)_5(NH_2C_6H_{11})$ a shift in the ν(NH) frequencies to lower wavenumbers occurred (see Figure 1) with concomitant changes in the infrared spectral properties in the ν(CO) region (Table II and Figure 2). As noted in Figure 1 for $Mo(CO)_5(NHC_5H_{10})$·$OP(n$-

Table I. Frequency Shifts of ν(NH) for $M(CO)_5$(amine) Species in the Presence of Lewis Bases[a]

M	coordinated amine	base	ν(NH), cm^{-1}	$\Delta\nu$(NH), cm^{-1}
Mo	$C_5H_{10}NH$	...	3270	...
		C_6D_6	3252	18
		$(C_6H_5)_3P$	3252	18[b]
		$(C_6H_5)_3PO$	3232	38
		C_4H_8ONH	3230	40
		THF	3222	48
		$(CH_3O)_3PO$	3211	59
		NH_3	3169	101
		$(n\text{-}C_4H_9)_3P$	3158	112
		C_5H_5N	3162	108
		$(n\text{-}C_4H_9)_3PO$	3158	112
		$C_5H_{10}ND$	3128	142
	$C_5H_{10}ND$	...	2416	...
		$(n\text{-}C_4H_9)_3PO$	2343	73
W	$C_5H_{10}NH$	...	3267	...
		C_6D_6	3248	19
		$(C_6H_5)_3P$	3246	21[b]
		$(C_6H_5O)_3P$	3219	48
		THF	3208	59
		$(CH_3O)_3PO$	3197	70
		$(C_2H_5O)_3P$	3196	71
		$(C_6H_5)_3PO$	3161	106
		$(n\text{-}C_4H_9O)_3P$	3155	112
		NH_3	3152	115
		$(CH_3)_2C_6H_5P$	3150	117
		$(n\text{-}C_4H_9)_3P$	3142	125
		$(n\text{-}C_4H_9)_3PO$	3140	127
		C_5H_5N	3138	129
		$(C_6H_{11})_3P$	3134	133
		$C_5H_{10}NH$	3106	161
Cr	$C_5H_{10}NH$	...	3273	...
		$(C_6H_5)_3P$	3253	20[b]
		C_5H_5N	3167	106
		$(C_6H_{11})_3P$	3159	114
		$(n\text{-}C_4H_9)_3PO$	3163	133
	$C_6H_{11}NH_2$[c]	...	3330	...
			3283	...
		$(C_6H_5)_3PO$	3228	102
			3146	137
		$(n\text{-}C_4H_9)_3PO$	3226	104
			3132	151

[a] Spectra observed in C_2Cl_4 in 1-mm solution cells. [b] Solution saturated with $P(C_6H_5)_3$. [c] Symmetric and asymmetric modes.

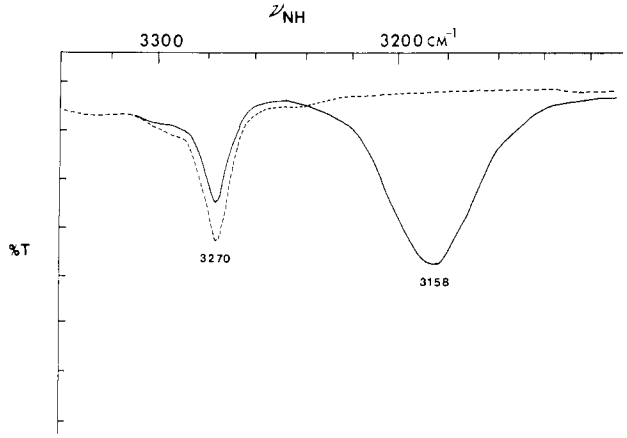

Figure 1. Infrared spectra in the ν(N–H) region in C_2Cl_4: (---) spectrum of pure $Mo(CO)_5NHC_5H_{10}$; (—) spectrum of $Mo(CO)_5NHC_5H_{10}$ with added $OP(n\text{-}C_4H_9)_3$.

(10) Normant, M. H.; Cuvigny, T.; Reisdorf, D. *C. R. Hebd. Seances Acad. Sci., Ser. C* **1969**, *268*, 521.
(11) Cuvigny, T.; Normant, M. H. *C. R. Hebd. Seances Acad. Sci., Ser. C* **1969**, *268*, 834.
(12) Williams, R. C.; Taylor, J. W. *J. Chem. Educ.* **1970**, *47*, 129.
(13) Ramette, R. W. *J. Chem. Educ.* **1967**, *44*, 647.
(14) Cotton, F. A.; Kraihanzel, C. S. *J. Am. Chem. Soc.* **1962**, *84*, 4432.

Table II. ^{12}CO Stretching Frequencies for $M(CO)_5$(amine) Compounds and Hydrogen-Bonded $M(CO)_5$(amine)·base Species[a]

complex	freq, cm^{-1} $A_1^{(2)}$	$A_1^{(1)}$	E
$Mo(CO)_5$pip	2073	1921	1939
$Mo(CO)_5$pip·$OP(n\text{-}C_4H_9)_3$	2066	1906	1930
$Mo(CO)_5$pip·$P(n\text{-}C_4H_9)_3$	2066	1906	1930
$Mo(CO)_5$pip·$OP(OCH_3)_3$		1908	1933
$Mo(CO)_5$pip·py		1910	1935
$Mo(CO)_5$pip·THF[b]		1908	1934
$Mo(CO)_5NH_3$		1921	1942
$Mo(CO)_5NH_3(THF)_n$[c]	2061	1879	1921
$Mo(CO)_5NH_2C_6H_{11}$	2076	1920	1940
$Mo(CO)_5NH_2C_6H_{11}$·$OP(n\text{-}C_4H_9)_3$	2071	1905	1931
$Cr(CO)_5$pip	2069	1916	1933
$Cr(CO)_5$pip·$OP(n\text{-}C_4H_9)_3$	2063	1901	1925
$Cr(CO)_5$pip·THF[d]	2064	1889	1920
$Cr(CO)_5$pip·$(CH_3)_2CO$[d]	2065	1881	1928
$W(CO)_5$pip	2074	1918	1928
$W(CO)_5$pip·$OP(n\text{-}C_4H_9)_3$	2069	1900	1920

[a] Frequencies were determined in hexane solutions with base concentrations of about 0.1 M; except where noted otherwise, they are accurate to ±1 cm^{-1}. pip = piperidine. [b] Two drops of THF in 5 mL of hexane. [c] THF as solvent: Fischer, E. O.; Bathlet, W.; Muller, J. *Chem. Ber.* **1971**, *104*, 986. [d] Base used as the solvent.

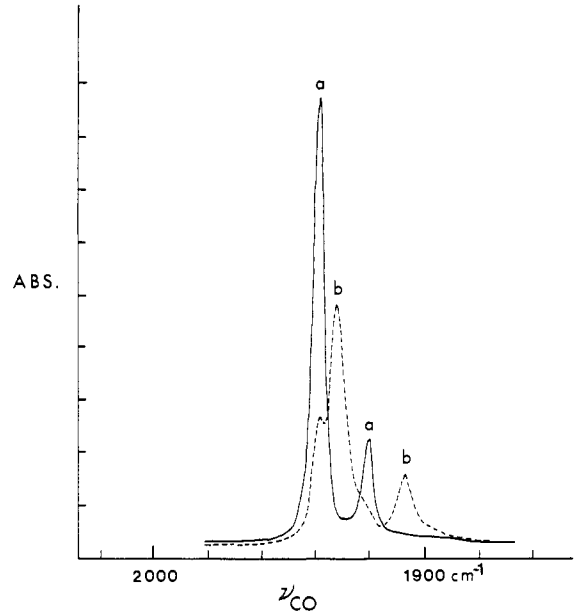

Figure 2. Infrared spectra in the ν(CO) region in hexane: (—) spectrum of pure $Mo(CO)_5NHC_5H_{10}$; (- - -) spectrum of $Mo(CO)_5NHC_5H_{10}$ with added $(n\text{-}C_4H_9)_3PO$. Bands labeled a and b correspond to the E and A_1 CO stretching modes in $Mo(CO)_5NHC_5H_{10}$ and $Mo(CO)_5NHC_5H_{10}$·$OP(n\text{-}C_4H_9)_3$, respectively.

$C_4H_9)_3$ the ν(NH) frequency shifts were accompanied by an enhancement (by a factor of ~8) in the intensity of the shifted ν(NH) vibration. Increases in the bandwidth at half-height of these shifted ν(NH) bands were also observed. A deuterated analogue, $Mo(CO)_5NDC_5H_{10}$ (ν(NH)/ν(ND) = 1.353), exhibited a shift to lower frequency upon addition of tri-*n*-butylphosphine oxide (ν(NH···O)/ν(ND···O) = 1.348). The theoretical ratio of ν(NH)/ν(ND), as calculated by the Teller–Redlich product rule, is 1.369.

The magnitude of the frequency shifts generally increased with increasing basicity as judged by the bases' ΔHNP values.[15,16] An exception to this was triphenylphosphine, which consistently resulted in frequency shifts as small as those of benzene.[17] The C_{4v} structure about the $M(CO)_5$ fragment persists in solution when the hydrogen-bonding interactions occurred, as indicated by the ν(CO) band patterns. For example, the ν(CO) frequencies of $Mo(CO)_5NHC_5H_{10}$ in excess $(n\text{-}C_4H_9)_3P{=}O$ were found at 2066, 1930, and 1906 cm^{-1} as compared to 2073, 1939, and 1921 cm^{-1} in the absence of phosphine oxide (Figure 2). These frequencies correspond to the $A_1^{(2)}$, E, and $A_1^{(1)}$ vibrational modes, respectively. The changes in ν(CO) upon hydrogen-bond formation in each case showed that the vibration ascribed mainly to the CO group trans to the amine (the $A_1^{(1)}$ mode) experienced a significantly greater frequency shift than the other vibrational modes. This effect is better illustrated when viewing the differences in CK force constant parameters upon hydrogen-bond formation (Table III).

The changes in ν(CO) and ν(NH) for $Mo(CO)_5NHC_5H_{10}$ in the presence of Lewis bases were accompanied by a simultaneous decrease in the wavelength of the band centered at ~400 mm in the visible spectrum ($A_1(b_2^2e^4) \rightarrow {}^1E(b_2^2e^3a^1)$ transition) by 40 Å (Figure 3). This slight increase in energy and the corresponding decrease in ν(CO) vibrations are both consistent with the expected increase in electron donation by the amine upon hydrogen-bond formation.

B. Reproducibility of, and Effects of Light on, k_1 and k_2. The thermal decomposition of $Mo(CO)_5NHC_5H_{10}$ to afford $Mo(CO)_6$ and its reaction with PPh_3 to provide $Mo(CO)_5PPh_3$ were studied kinetically under a variety of reaction conditions at 34.5 °C in hexane. The reproducibility of the rate in general, the possible catalytic or inhibitory effects of species generated during decomposition and PPh_3 substitution reactions, and the reliability of determining the rate constant by an initial rate method[4] in which only the first 10% of the reaction is monitored, were investigated. The results are summarized in Table IV. As noted in Table IV the first-order rate constants for piperidine dissociation measured under various conditions were closely reproducible.

Further it was shown that starting with an approximately 1:1 molar ratio of starting material to NHC_5H_{10} or $Mo(CO)_6$ had no apparent effect on k_1. Moreover, saturation of the reaction solution with carbon monoxide and following either $Mo(CO)_6$ formation or $Mo(CO)_5NHC_5H_{10}$ disappearance gave rate constants compatible with the range of experimental uncertainties for decomposition of freshly prepared and purified $Mo(CO)_5NHC_5H_{10}$.

It has been amply demonstrated that $Mo(CO)_5NHC_5H_{10}$ undergoes photosubstitution of the amine moiety in solution.[18,19] The photosensitivity of the piperidine ligand substitution process upon exposure to the overhead fluorescent lighting and to the monitoring of the reactions with visible light in reactions with PPh_3 in hexane was estimated. The kinetic results are reported in Tables V and VI. The piperidine thermal substitution reactions obeyed the normal empirical rate law (eq 2) under the pseudo-first-order conditions (excess PPh_3) in both the presence and the absence of a light source.

The k_1 and k_2 values reported in Table VI were obtained by least-squares analysis of the rate-constant expression given in eq 2. As noted in Table VI, the k_1 parameter is larger in the presence of visible light, and it is this rate enhancement that accounts for the discrepancy in our earlier report of this rate parameter where care was not taken to avoid exposure

(15) Streuli, C. A. *Anal. Chem.* **1959**, *31*, 1652.
(16) Streuli, C. A. *Anal. Chem.* **1960**, *32*, 985.

(17) Upon addition of excess quantities of aliphatic phosphines to solutions of $M(CO)_5NHC_5H_{10}$, shifts in ν(NH) and ν(CO) similar to those for the corresponding phosphine oxides were observed. Although the origins of these shifts are somewhat uncertain, they are believed to be due to trace impurities of the oxide species, which are exceptionally good hydrogen-bonding bases.
(18) Wrighton, M. *Inorg. Chem.* **1974**, *13*, 905.
(19) Darensbourg, D. J.; Murphy, M. A. *Inorg. Chem.* **1978**, *17*, 884.

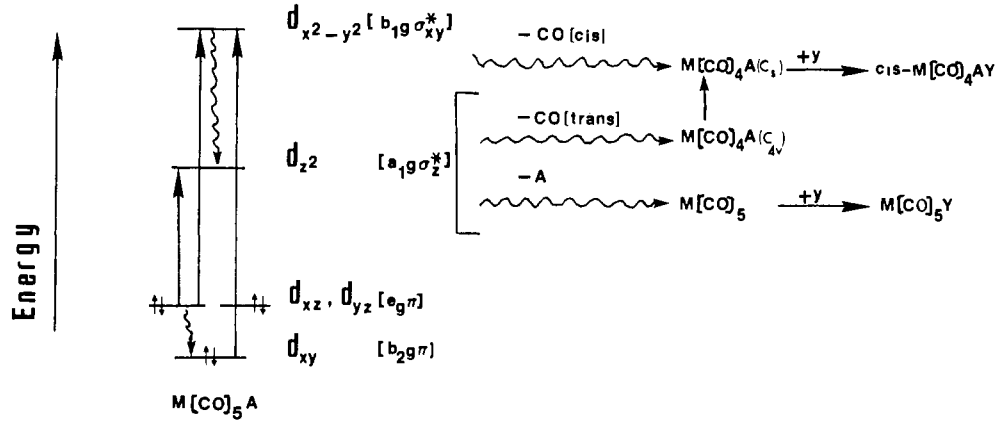

Figure 3. Orbital diagram for visible and ultraviolet absorption transitions in group 6B $M(CO)_5$(amine) species.

Table III. Variation of Frequencies and Calculated CO Stretching Force Constants upon Hydrogen-Bond Formation between N-H Groups of $M(CO)_5NHC_5H_{10}$ Species and Lewis Bases in Hexane

complex	base	freq, cm^{-1}			force constants,[a] mdyn A^{-1}				
		$A_1^{(2)}$	$A_1^{(1)}$	E	k_1	k_2	k_i	Δk_1[b]	Δk_2[b]
$Mo(CO)_5NHC_5H_{10}$	...	2073	1921	1939	15.10	15.86	0.33	0.00	0.00
	$(n\text{-}C_4H_9)_3PO$	2066	1906	1930	14.87	15.72	0.33	−0.23	−0.14
$Cr(CO)_5NHC_5H_{10}$	...	2068	1916	1932	15.03	15.75	0.33	0.00	0.00
	$(n\text{-}C_4H_9)_3PO$	2063	1901	1925	14.80	15.66	0.34	−0.23	−0.09
	THF[c]	2063	1889	1920	14.61	15.61	0.35	−0.42	−0.05
	acetone[c]	2065	1881	1928	14.46	15.70	0.34	−0.57	−0.05
$W(CO)_5NHC_5H_{10}$	...	2073	1918	1928	15.08	15.73	0.35	0.00	0.00
	$(n\text{-}C_4H_9)_3PO$	2069	1900	1920	14.80	15.62	0.36	−0.28	−0.11

[a] These were calculated by the method as described in ref 14. [b] Force constant difference between adduct and free complex, where k_1 and k_2 correspond to the axial and equatorial CO stretching force constants, respectively. [c] Base used as the solvent. Data taken from ref 3.

Table IV. First-Order Rate Constants for Piperidine Dissociation from $Mo(CO)_5NHC_5H_{10}$ in Hexane

condition tested for influence on k_1	temp, °C	10^5k_1, s^{-1}
purified $Mo(CO)_5NHC_5H_{10}$ alone (80% completion)	34.5	1.50
~1:1 $Mo(CO)_5NHC_5H_{10}/Mo(CO)_5P(C_6H_5)_3$ initially	34.5	1.51
50 mg/25 mL of insoluble decomposition products from other solution reactions added initially	34.5	1.60
$Mo(CO)_5NHC_5H_{10}$ used was discolored on storage	34.5	1.48
k_1 by extrapolation to zero $P(C_6H_5)_3$ concentration for pseudo-first-order ligand substitution reactions	34.5	1.58
mean of rate constants above	34.5	1.53
rate from first 10% of decomposition only	34.5	1.68

Table V. Pseudo-First-Order Rate Constants for Reaction of $Mo(CO)_5NHC_5H_{10}$ with $P(C_6H_5)_3$ in Hexane at 34.5 °C

reactn protected from light		reactn exposed to overhead fluorescent light	
$10^3 \times [P(C_6H_5)_3]$, M	10^5k_{obsd}, s^{-1}	$10^3 \times [P(C_6H_5)_3]$, M	10^5k_{obsd}, s^{-1}
	1.50		3.96
3.00	1.90		
10.00	2.30	10.0	5.18
20.00	2.62		
25.2	3.06	21.5	6.40
30.0	3.71		

of the sample to room lighting during the kinetic runs.[3,20] Interestingly, the k_2 values suggest that the second-order term also exhibits photosensitivity. The number of known bimolecular excited-state substitution pathways stands in contrast

(20) The activation parameters were however in agreement with the corresponding values determined in the absence of light.

Table VI. First- and Second-Order Rate Constants for $P(C_6H_5)_3$ Substitution of Amine in $Mo(CO)_5NHC_5H_{10}$ in Hexane

light source	10^5k_1, s^{-1}	10^4k_2, M^{-1} s^{-1}	T, °C
overhead fluorescent	3.96[a]	11.3	34.5
Cary 14 spectrophotometer[b]	1.84	12.4	35
none	1.58	6.38	34.5

[a] A value of 3.73×10^{-5} s^{-1} was reported for a reaction carried out with overhead lighting: Dennenberg, R. J.; Darensbourg, D. J. *Inorg. Chem.* 1972, *11*, 72. [b] Data from: Covey, W. D.; Brown, T. L. *Inorg. Chem.* 1973, *12*, 2820.

to the many dissociative photosubstitution reactions that have been documented. However, there have been a few previous reports of evidence for this type of behavior with substituted metal carbonyl derivatives.[21]

C. Reactions of $M(CO)_5NHC_5H_{10}$ (M = Cr and Mo) with $P(n\text{-}C_4H_9)_3$. The measured rate constants for $P(n\text{-}C_4H_9)_3$ substitution reactions with $Mo(CO)_5NHC_5H_{10}$ are summarized in Table VII. The results for $Mo(CO)_5NHC_5H_{10}$ at 34.5 °C are shown graphically in Figure 4. The rates for $Mo(CO)_5NHC_5H_{10}$ conform to the rate constant expression given in eq 13 for a dissociative-interchange mechanism. k_1 was determined by an analysis according to the inverted linear form of eq 13 and was found to vary considerably for runs at comparable temperatures. Even triple vacuum distillations of the $(n\text{-}C_4H_9)_3P$ did not eliminate this erratic kinetic behavior, although it was apparent that results were more self-consistent when $(n\text{-}C_4H_9)_3P$ of the highest purity was employed.

The rates for $Cr(CO)_5NHC_5H_{10}$ reactions with $(n\text{-}C_4H_9)_3P$ showed little variation with increasing $(n\text{-}C_4H_9)_3P$ concen-

(21) Vogler, A. In "Concepts of Inorganic Photochemistry"; Adamson, A. W., Fleischauer, P. D., Eds.; Wiley-Interscience: New York, 1975; Chapter 6.

Table VII. Pseudo-First-Order Rate Constants, Apparent "K_1" Values, and Maximum Rates for $Mo(CO)_5NHC_5H_{10}$ and $P(n\text{-}C_4H_9)_3$[a]

T, °C	$10^3 \times [(n\text{-}C_4H_9)_3P]$,[b] M	$10^4 k_{obsd}$, s^{-1}	"K_1",[c] M^{-1}	$10^4 k_{max}$,[c] s^{-1}
14.9	99.0	0.726	197 ± 11	0.761 ± 0.14
	19.8	0.603		
	9.90	0.504		
23.9	100	2.45	68.2 ± 7.5	2.75 ± 0.26
	30	1.81		
	10	1.12		
25.2	198	4.20	157 ± 30	4.04 ± 0.82
	99	4.06		
	39.6	3.64		
	29.7	3.36		
	19.8	3.08		
	9.90	2.41		
	4.95	1.52		
	2.48	1.19		
34.5	99.0	8.39	213 ± 35	8.35 ± 1.12
	39.6	8.12		
	29.7	7.20		
	19.8	6.82		
	9.90	5.36		
	4.95	3.95		
	2.48	2.98		
42.3	99.0	15.1	178 ± 34	16.9 ± 4.2
	9.90	11.8		
	4.95	7.59		
	2.48	5.18		
43.6	99.0	18.7	72	21.4
	29.7	15.0		
	19.8	13.1		
	9.9	8.35		
	4.95	5.72		

[a] The concentration of the impurity, $OP(n\text{-}C_4H_9)_3$, contained in each solution is unknown. [b] These concentrations are only approximate due to oxidation of the ligand. [c] Confidence limits of 95%.

tration over the range investigated (0.020–0.253 M). This is consistent with the ν(CO) region of the infrared spectra of these reaction solutions, which indicated approximately complete conversion of $Cr(CO)_5NHC_5H_{10}$ to the outer-sphere complex, $Cr(CO)_5NHC_5H_{10}\cdot OP(n\text{-}C_4H_9)_3$.

The kinetic behavior of $Cr(CO)_5NHC_5H_{10}$ and $Mo(CO)_5NHC_5H_{10}$ with $P(n\text{-}C_4H_9)_3$ is felt to be due to a general-base-catalysis mechanism by varying amounts of $OP(n\text{-}C_4H_9)_3$ present as an impurity. This view is further supported by the infrared spectra and kinetics of solutions in reactions of the Cr, Mo, and W piperidine derivatives with $OP(n\text{-}C_4H_9)_3$ and PPh_3 described in the following section. Small amounts of disubstituted products (≤5% of total product) were formed in some tri-*n*-butylphosphine reactions. These derivatives arise as a consequence of the CO-labilizing ability of the $OP(n\text{-}C_4H_9)_3$ ligand in the $M(CO)_5OP(n\text{-}C_4H_9)_3$ intermediates.[22]

D. Thermal Decomposition and Ligand Substitution Reactions between $M(CO)_5NHC_5H_{10}$ (M = Cr, Mo, or W) and PPh_3 in the Presence of $OP(n\text{-}C_4H_9)_3$. The kinetic results for the reactions of these piperidine derivatives with PPh_3 in hexane solution were reproducible and were unaffected by the addition of $OPPh_3$ owing to the insolubility of this oxide in hexane.[23,24] The effects of adding known concentrations of $OP(n\text{-}C_4H_9)_3$ to reaction solutions of the piperidine derivatives

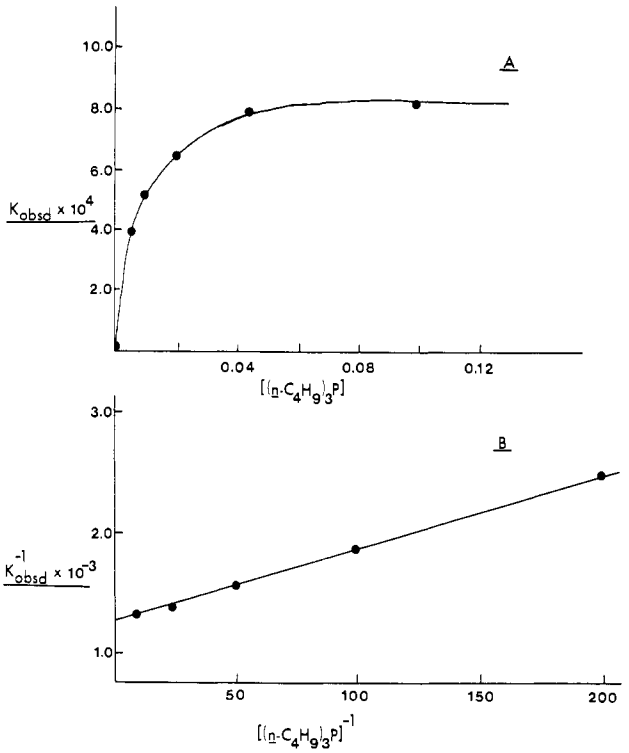

Figure 4. (A) Observed rate constant vs. $[(n\text{-}C_4H_9)_3P]$ for the reaction of $Mo(CO)_5NHC_5H_{10}$ with $(n\text{-}C_4H_9)_3P$. (B) Double-reciprocal plot for the reaction of $Mo(CO)_5NHC_5H_{10}$ with $(n\text{-}C_4H_9)_3P$.

Table VIII. Pseudo-First-Order Rate Constants for $Mo(CO)_5NHC_5H_{10}$ and $P(C_6H_5)_3$ Substitution Reactions as a Function of $(C_6H_5)_3P$ and $(n\text{-}C_4H_9)_3PO$ Concentrations at 34.5 °C

$10^3 \times [(n\text{-}C_4H_9)_3PO]$, M	$10^2 \times [(C_6H_5)_3P]$, M	$10^4 k_{obsd}$,[a] s^{-1}
		0.152
0.451	5.01	2.83 ± 0.08
0.808	2.08	3.58 ± 0.06
1.15	1.25	4.22 ± 0.17
2.30	2.50	6.06 ± 0.22
4.60	5.01	7.92 ± 0.32
6.90	7.52	8.39 ± 0.39
9.20	10.00	9.00 ± 0.31

[a] Confidence limits of 95%; $k_c = (1.04 \pm 0.09) \times 10^{-3}$ s^{-1} and $K_c = 633 \pm 54$ M^{-1}.

Table IX. Pseudo-First-Order Rates of Piperidine Substitution for $W(CO)_5NHC_5H_{10}$ with $P(C_6H_5)_3$ Showing Catalysis by $OP(n\text{-}C_4H_9)_3$ at 60.3 °C

$10^2 \times [P(C_6H_5)_3]$, M	$10^2 \times [OP(n\text{-}C_4H_9)_3]$, M	$10^4 k_{obsd}$,[a] s^{-1}
2.22		0.130 ± 0.001
2.22	1.04[b]	1.01 ± 0.02

[a] Confidence limits of 95%. [b] Corresponds to complete adduct formation for $W(CO)_5NHC_5H_{10}\cdot OP(n\text{-}C_4H_9)_3$.

in decomposition runs and ligand substitution reactions with PPh_3 were observed to determine if this $P(n\text{-}C_4H_9)_3$ oxidation product[25] could be responsible for the anomalous kinetic behavior in the reactions with $P(n\text{-}C_4H_9)_3$ (vide supra). The kinetic results for Mo, W, and Cr are collected in Tables VIII, IX, and X, respectively. All the reactions obeyed the rate

(22) (a) Darensbourg, D. J.; Walker, N.; Darensbourg, M. Y. *J. Am. Chem. Soc.* **1980**, *102*, 1213. (b) Darensbourg, D. J.; Darensbourg, M. Y.; Walker, N. *Inorg. Chem.* **1981**, *20*, 1918.

(23) On the other hand, $OPPh_3$ has been shown to account for the irreproducibility in kinetic studies of the reaction of $W(CO)_5(NH_2Ph)$ with PPh_3 in toluene where the triarylphosphine oxide is soluble.[24]

(24) Nasielski, J.; Vermeulen, M.; Leempoel, P. *J. Organomet. Chem.* **1975**, *102*, 195.

(25) Wiberg, K. B. "Physical Organic Chemistry"; Wiley: New York, 1964; p 570.

Table X. Pseudo-First-Order Rate Constants for $Cr(CO)_5NHC_5H_{10}$ Decomposition and $P(C_6H_5)_3$ Substitution Reactions as a Function of $(C_6H_5)_3P$ and $(n\text{-}C_4H_9)_3PO$ Concentrations and Reaction Temperatures

T, °C	$10^3 \times$ $[(n\text{-}C_4H_9)_3PO]$, M	$10^3 \times$ $[PPh_3]$, M	$10^5 k_{obsd}$,[a] s^{-1}	$10^5 k_c$,[a] s^{-1}	K_c,[a] M^{-1}
34.5	96.2	45.6	6.46 ± 0.20	6.61 ± 0.21	566 ± 53
	9.62	45.6	5.70 ± 0.14		
	7.70	45.6	5.32 ± 0.16		
	4.81	45.6	4.82 ± 0.17		
	2.89	45.6	4.11 ± 0.21		
44.5	11.6	...	23.8 ± 0.87	26.5 ± 3.7	502 ± 121
	7.70	...	20.6 ± 0.40		
	4.81	...	18.1 ± 0.26		
	1.92	...	13.1 ± 0.14		
54.5	11.6	...	71.3 ± 1.2	83.1 ± 4.8	509 ± 112
	7.70	...	65.8 ± 2.3		
	5.78	...	62.2 ± 1.5		
59.7	192	45.6	144 ± 3.2	145 ± 4	444 ± 45
	23.2	45.6	132 ± 4.8		
	15.4	45.6	128 ± 1.4		
	9.62	45.6	115 ± 4.5		
	3.84	45.6	91.7 ± 2.6		
50.1	...	...	10.1 ± 0.16		
57.4	...	...	24.9 ± 1		

[a] Uncertainties are 95% confidence limits.

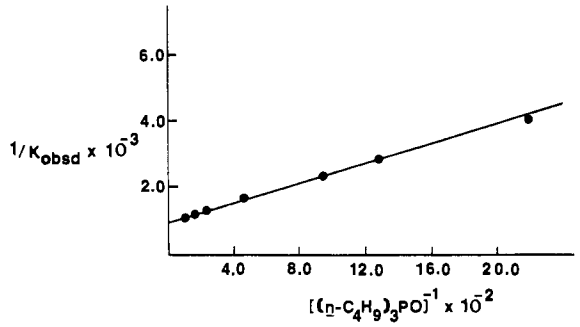

Figure 5. Double-reciprocal plot according to eq 20 for the reaction of $Mo(CO)_5NHC_5H_{10}$ with PPh_3 in the presence of $(n\text{-}C_4H_9)_3PO$ in hexane at 34.5 °C.

constant expressions given in eq 19 and 20 for the general-base-catalyzed mechanism over most of the concentration range studied as is depicted for the $Mo(CO)_5NHC_5H_{10}$ reactions at 34.5 °C in Figure 5.

The formation constant for $Mo(CO)_5NHC_5H_{10}\cdot OP(n\text{-}C_4H_9)_3$ calculated from the kinetic data was 633 ± 54 M^{-1} (95% confidence limits), and the maximum rate constant (k_c), obtained by extrapolation to $1/[OP(n\text{-}C_4H_9)_3]$ = zero, was $(1.04 \pm 0.09) \times 10^{-3}$ s^{-1} at 34.5 °C. The rate at the lowest phosphine oxide concentration was omitted from the above analysis because eq 20 is probably only an approximation for the complete rate constant expression (eq 21). Inspection of the data in Figure 5 shows qualitatively that the rate constant determined at the lowest phosphine oxide concentration differs from that predicted by eq 20 ($k_{calcd} = 2.45 \times 10^{-4}$ s^{-1}; $k_{obsd} = (2.83 \pm 0.08) \times 10^{-4}$ s^{-1}). Since K_1 is too small for a reliable estimate and $K_1[B] \ll 1$, eq 21 can be reduced to the approximate expression in eq 22. Equation 22 predicts $k_{calcd} = 2.68 \times 10^{-4}$ s^{-1}, which is in fairly close agreement with the observed rate and supports the mechanism depicted in Scheme I.

$$k_{obsd} = \frac{k_1 + k'_2K_1[B] + k_cK_c[C]}{1 + K_c[C]} \qquad (22)$$

If the spurious data point is included in the least-squares analysis by eq 20, this results in K_c = 923 ± 183 M^{-1} and changes the reciprocal of the intercept (k_c) to $(9.11 \pm 2.02) \times 10^{-4}$ s^{-1}. These changes testify to how very sensitive this type of analysis can be to the valid range for the inherent assumptions made in the kinetic treatment.

A semiquantitative estimate of K_c was made with use of Ramette's method[13] (case I), which gave a value of $K_c = 1120 \pm 355$ M^{-1}. The rough spectrophotometric value corresponds to ~23 °C as the spectra were recorded at ambient temperature and extrapolated back to time = 0 s. The kinetic and spectrophotometric equilibrium constants agree within experimental error despite the semiquantitative nature of the latter determination.

Reactions were carried out between $W(CO)_5NHC_5H_{10}$ and PPh_3 in both the presence and the absence of $OP(n\text{-}C_4H_9)_3$ in order to observe if the oxide had a similar catalytic effect with the tungsten derivative (Table IX). The approximately 8-fold increase in rate for amine substitution in the tungsten analogue upon the addition of phosphine oxide (60.3 °C), as compared to about a 68-fold increase for the corresponding process for the molybdenum derivative (34.5 °C), shows the catalytic effect of the phosphine oxide to be more pronounced for the more labile molybdenum compound. Qualitatively, K_c for hydrogen bonding between the tungsten complex and the phosphine oxide appeared to be approximately the same as that for $Mo(CO)_5NHC_5H_{10}$.

The catalytic effects of $OP(n\text{-}C_4H_9)_3$ on piperidine dissociation were extended to include $Cr(CO)_5NHC_5H_{10}$ decomposition and substitution reactions with PPh_3 (Table X). The results obtained for chromium are analogous to those found for molybdenum and tungsten. The rate of piperidine dissociation in $Cr(CO)_5NHC_5H_{10}$ at 50.1 °C is estimated to be increased by about a factor of 5 as compared to a factor of about 68 for molybdenum at 34.5 °C.

The equilibrium constants for formation of $Cr(CO)_5NHC_5H_{10}\cdot OP(n\text{-}C_4H_9)_3$ are only slightly less than those for the molybdenum complex. From the slope of ln K_c vs. $1/T$, $\Delta H°$ was calculated to be ~−2 kcal/mol for the equilibrium described in eq 23. Both the exothermicity and the magnitude

$$Cr(CO)_5NHC_5H_{10} + OP(n\text{-}C_4H_9)_3 \rightleftharpoons Cr(CO)_5NHC_5H_{10}\cdot OP(n\text{-}C_4H_9)_3 \qquad (23)$$

of $\Delta H°$ are compatible with the measured equilibrium process being due to hydrogen bonding.[26,27]

An attempt was made to measure K_c for reaction 23 spectrophotometrically at 24.5 °C where the amine substitution

(26) Green, R. D. "Hydrogen Bonding by C-H Groups"; Wiley: New York, 1974.
(27) Pimentel, G. C.; McClellan, A. L. "The Hydrogen Bond"; W. H. Freeman: New York, 1960.

Table XI. Data Used for Spectrophotometric Determination of K_{eq} for $Cr(CO)_5NHC_5H_{10}\cdot OP(n\text{-}C_4H_9)_3$ at 24.5 °C in Hexane[a]

$10^2 \times [OP(n\text{-}Bu)_3]_i$, M	$10^{-3}E_{app}$ (1933 cm^{-1}), $cm^{-1}\ M^{-1}$	$10^2 \times [OP(n\text{-}Bu)_3]_e$,[b] M	K_{eq}, M^{-1}
0.481	23.1	0.448	523
0.722	19.8	0.664	748
0.962	18.2	0.892	744
1.92	14.1	1.81	734
2.89	11.9	2.77	716
3.85	10.6	3.72	684
4.81	9.31	4.67	734
7.70	7.94	7.55	659
11.60	7.29	11.4	537
			av = 675 ± 66

[a] Subscripts i and e indicate initial and calculated equilibrium concentrations. E_{app} is the apparent absorptivity of the solution at the E mode for $Cr(CO)_5NHC_5H_{10}$. Complex initial concentration was 1.7×10^{-3} M for all solutions. The extinction coefficients for the complex and the adduct were 27 600 and 3990 $cm^{-1}\ M^{-1}$, respectively. [b] Obtained by the procedure described in ref 13.

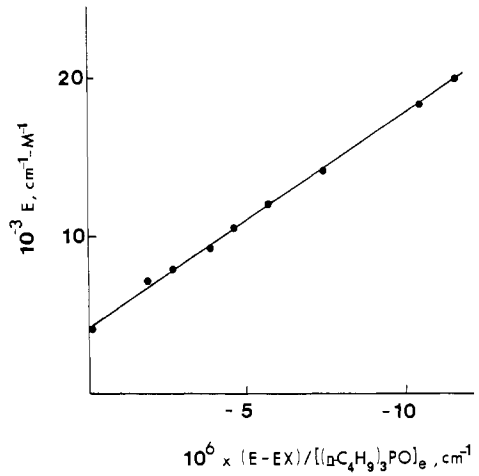

Figure 6. K_c plot for the formation of $Cr(CO)_5(NHC_5H_{10})\cdot OP(n\text{-}C_4H_9)_3$.

was sufficiently slow such that extrapolation to time zero was unnecessary. This determination is described in the following section. The independently determined spectrophotometric equilibrium constant is 675 ± 66 M^{-1} as compared to the kinetic value extrapolated to the same temperature of 627 M^{-1}.

E. Spectroscopic Determination of K_c for Formation of $Cr(CO)_5NHC_5H_{10}\cdot OP(n\text{-}C_4H_9)_3$. The procedure employed in the spectrophotometric determination of the K_c value for reaction 23 was as described by Ramette.[13] The data for the ascertainment of K_c are summarized in Table XI and plotted in Figure 6, where E is the apparent absorptivity of the solution and EX is the extinction coefficient of $Cr(CO)_5NHC_5H_{10}$ measured at 1933 cm^{-1} (the ν(CO) E mode in $Cr(CO)_5NHC_5H_{10}$). The negative value of the reciprocal of the slope of the plot in Figure 6 corresponds to K_c, with the intercept being the molar absorptivity of the adduct $Cr(CO)_5NHC_5H_{10}\cdot OP(n\text{-}C_4H_9)_3$. K_c was found to be 675 ± 66 M^{-1}, and the zero intercept (4300 $cm^{-1}\ M^{-1}$) agreed closely with the extinction coefficient measured for $Cr(CO)_5NHC_5H_{10}\cdot OP(n\text{-}C_4H_9)_3$ (3990 $cm^{-1}\ M^{-1}$) from Beer's law plots in solutions containing an excess of $OP(n\text{-}C_4H_9)_3$. The good linearity of the plot in Figure 6 testifies to the absence of complicating equilibria.[13]

In addition, investigation of the phosphoryl stretching region in the infrared spectra of the fairly dilute hexane solutions of $OP(n\text{-}C_4H_9)_3$ employed in these kinetic studies showed no evidence for any other equilibria.

Table XII. Solvent Effects on the Rate of Decomposition of $Mo(CO)_5$pip at 44.8 °C

solvent	10^5k_1, s^{-1}	E^a
benzene	2.53	2.284
m-xylene	3.52	2.374
chlorobenzene	4.52	5.708
hexane	5.93	1.890
cyclohexene	11.45	2.220
chloroform	20.58	4.806
nitromethane	21.40	34.80
carbon disulfide	25.40	2.641
1,4-dioxane	27.67	2.209
cyclohexanone	59.80	18.300

[a] Dielectric constant at 20 °C: Riddick, J. A.; Bunger, W. B. In "Techniques of Organic Chemistry"; Weissberger, A., Ed.; Wiley-Interscience: New York, 1970; Vol. 2.

Table XIII. Rate Constants for $Mo(CO)_5$pip Substitution Reactions with Triphenylphosphine in THF as a Function of Temperature[a]

T, °C	$10^2[P(C_6H_5)_3]$, M	10^4k_{obsd}, s^{-1}
35		1.16
43.4	5.17	3.37
49.1	5.12	6.22
49.1	10.2	6.21

[a] Activation parameters and their 95% confidence limits are $\Delta H^* = 23.0 \pm 2.1$ kcal mol^{-1} and $\Delta S^* = -1.9 \pm 6.8$ eu.

F. Solvent Effects on the Thermal Decomposition of $Mo(CO)_5NHC_5H_{10}$ and Its Substitution Reactions with PPh_3. Table XII lists the effects of 10 solvents on the rate of decomposition of $Mo(CO)_5NHC_5H_{10}$ at 44.8 °C. There is little dependence of k_1 on the solvents' dielectric constants. The most rapid rates were found for solvents that are known to be good electron-pair donors for hydrogen bonding,[26,27] with the bulkiest of these generally giving the faster rates of dissociation. The π-electron-cloud donors appear to decrease the rates relative to hexane. This latter effect may be due to stabilization of $Mo(CO)_5NHC_5H_{10}$ through a specific solvent interaction.

For a better understanding of both the solvent effects on the thermal decompositions and their effects on the mechanisms of ligand substitution,[4] more detailed investigations on the influence of added Lewis bases and mixed solvents in which one solvent was a Lewis base were made.

Ligand substitution reactions between $Mo(CO)_5NHC_5H_{10}$ and PPh_3 were examined with use of solvent mixtures of hexane and tetrahydrofuran, and in tetrahydrofuran alone. THF appeared to be a weak catalyst for the ligand-exchange process. The rate of amine dissociation in THF was only ~10 times faster than in hexane (Table XIII). Studies with hexane as the solvent and with added THF varying from 0.12 to 1.2 M were in accord with a trend toward the rate increasing asymptotically to a maximum value close to that observed in THF alone at THF concentrations sufficiently high such that $k_1 + k'_2K_1[PPh_3] \ll k_cK_c[THF]$ (Figure 7, eq 20).

The reactions carried out in THF gave quantitative conversion to $Mo(CO)_5PPh_3$ as shown by Kezdy–Swimbourne plots[28] (eq 24). C_∞, C_n, and C_n' represent the concentrations

$$C_n = C_\infty[1 - \exp(k(\Delta t))] + C_n' \exp(k(\Delta t)) \quad (24)$$

of $Mo(CO)_5PPh_3$ at the infinity point and times t and $(t + t')$, respectively. These concentrations were determined by solving simultaneous equations employing the measured extinction coefficients of each of the overlapping bands of product and starting material in the solvent mixture at times t and $(t + t')$ (Δt = 20 min).

(28) Swinbourne, E. S. "Analysis of Kinetic Data", Nelson: London, 1971.

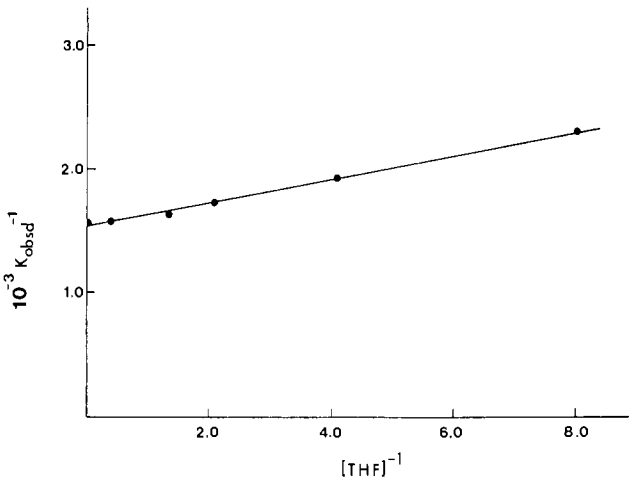

Figure 7. Double-reciprocal plot for the reaction of $Mo(CO)_5NHC_5H_{10}$ with PPh_3 in mixed solvents of hexane and THF at 49.1 °C.

G. Activation Parameters for $M(CO)_5NHC_5H_{10}$·B Outer-Sphere Complex Reactions, M = Cr or Mo and B = THF or $OP(n\text{-}C_4H_9)_3$. The activation parameters for the $M(CO)_5NHC_5H_{10}$·$OP(n\text{-}C_4H_9)_3$ outer-sphere complexes where M = Mo or Cr were calculated with use of the maximum extrapolated velocities (Figure 8 and Table XIV). The ΔH^* and ΔS^* values are compared with those for the thermal decomposition of the free $M(CO)_5NHC_5H_{10}$ complex in the same solvent. The activation parameters obtained for the outer-sphere complexes are consistent with the normal range for D processes involving metal carbonyl derivatives in general.[29-31]

H. Hydrogen-Bonding Effects on Cotton–Kraihanzel CO Stretching Force Constants in $M(CO)_{6-n}L_n$ Derivatives. Changes in frequencies in the CO stretching region of $M(CO)_5NHC_5H_{10}$ species in hexane on addition of Lewis bases that form hydrogen bonds to the N–H group and the calculated CO force constants are shown in Table III along with analogous solvent effects. The CO force constants were calculated according to the approximate method of Cotton and Kraihanzel[14] since these parameters are a more reliable measure of the CO bond strength than the CO frequencies. The band assignments in the CO stretching region listed in Table III for the free amine were made previously.[3] By analogy the relative positions and intensities of the bands suggest the assignments for the hydrogen-bonded adducts.[7] The changes in ν(CO) upon hydrogen-bond formation show that the vibration ascribed to the CO group trans to nitrogen exhibits a greater sensitivity.

This trans-directed influence of increasing the amine's basicity by hydrogen bonding may be a general phenomenon, for similar effects in group 6B *cis*-$L_2M(CO)_4$ species are noted.[32,33] Similarly, frequency shifts in *cis*-$Mo(CO)_4[PPh_3]NHC_5H_{10}$ were noted to be greater for the vibrational modes involving CO groups trans to the nitrogen donor, i.e., the $A_1^{(1)}$ and B_2 modes.

Discussion

The dissociation of the amine ligand in $Mo(CO)_5NHC_5H_{10}$ was found to be sufficiently photosensitive to indicate that discrepancies between the published rates resulted from photochemical effects.[3,4] A rationale for the photosensitivity of both incoming ligand-independent and -dependent pathways can be made with use of the widely adopted model for the photoreactions of metal carbonyl derivatives[18,19,34-36] and the proposal originally made by Covey and Brown[4] that the bimolecular thermal ligand substitution reactions for $Mo(CO)_5NHC_5H_{10}$ proceeds via concurrent D and I_d mechanisms.

The suggested photoprocesses that lead to excited states yielding ligand labilization along either the *xy* axis or the *z* axis are represented in Figure 3. Population of the σ_z^* ($^1A_1(b^2e^4) \rightarrow {}^1E(b^2e^3a^1)$) level for $Mo(CO)_5NHC_5H_{10}$, as a result of irradiation of the absorption band centered at 398 nm,[37-39] labilizes the exclusively σ-donor amine ligand in preference to the good π-acceptor CO ligand trans to the unique ligand.[19] The alternative possibility of population of the σ_{xy}^* ($^1A_1(b_2^2e^4) \rightarrow {}^1A_2(e^4b_2^1b_1^1)$ spin forbidden but orbitally allowed) due to absorption at a somewhat higher energy band (~340 nm), resulting in labilization of the equatorial CO groups, was not noticeable during this study.

The ligand dependence in the thermal and photochemical substitution reactions (k_2 in eq 3) has been proposed to be the product of a dissociative rate constant and an equilibrium constant (k'_2K_1, eq 14). Since there is a similarity between the rate-determining steps for both the D and I_d mechanisms, it is reasonable for the I_d path (k'_2 in eq 14) to exhibit photochemical behavior analogous to the D mechanism (k_1 in eq 6), and thus give rise to an *apparent* bimolecular excited-state substitution pathway. This would be anticipated particularly if the outer-sphere complex were isoelectronic and isostructural with the starting material. Indeed, the spectroscopic evidence suggests that a hydrogen-bonding interaction between the incoming ligand and the metal carbonyl complex is the most probable mode of interaction for the I_d process in this instance.

Although the association between the $Mo(CO)_5NHC_5H_{10}$ species and PPh_3 was too weak for identification of an intermediate, the evidence in this instance is overwhelmingly in favor of formation of a transient hydrogen-bonded outer-sphere complex. This is particularly so since THF (and other hydrogen-bonding solvents)[4] competes effectively with PPh_3 and quenches the bimolecular ligand substitutional pathway entirely. Thus eq 25–32 explain the delicate balance between

$$M(L)_nA + S \rightleftharpoons M(L)_nA\cdot S \quad (25)$$

$$M(L)_nA\cdot S \rightarrow M(L)_nS\cdot A \quad (26)$$

$$M(L)_nS\cdot A \rightarrow M(L)_nS + A \quad (27)$$

$$M(L)_nS \rightarrow M(L)_n + S \quad (28)$$

$$M(L)_n + B \rightarrow M(L)_nB \quad (29)$$

or

$$M(L)_nA + S' \rightleftharpoons M(L)_nA\cdot S' \quad (30)$$

$$M(L)_nA \rightleftharpoons M(L)_n + A \quad (31)$$

$$M(L)_n + B \rightarrow M(L)_nB \quad (32)$$

(29) Angelici, R. J. *Organomet. Chem. Rev., Sect. A* **1968**, *3*, 173.
(30) Dobson, G. R. *Acc. Chem. Res.* **1976**, *9*, 300.
(31) tomDieck, H.; Renck, I. W. *Angew. Chem., Int. Ed. Engl.* **1970**, *9*, 793.
(32) Data taken from ref 31.
(33) Jernigan, R. T.; Brown, R. A.; Dobson, G. R. *J. Coord. Chem.* **1972**, *2*, 47.
(34) Wrighton, M.; Hammond, G. S.; Gray, H. B. *Mol. Photochem.* **1973**, *5*, 179.
(35) Wrighton, M. *Chem. Rev.* **1974**, *74*, 401.
(36) Dahlgren, R. M.; Zink, J. I. *Inorg. Chem.* **1977**, *16*, 3154.
(37) Definitive analysis of the electronic excited states in $M(CO)_5$(amine) derivatives (M = Cr, Mo, W) has been obtained, using magnetic circular dichroism (MCD) spectroscopy.[38]
(38) Schreiner, A. F.; Amer, S.; Duncan, W. M.; Ober, G.; Dahlgren, R. M.; Zink, J. *J. Am. Chem. Soc.* **1980**, *102*, 6871.
(39) See also: Cotton, F. A.; Darensbourg, D. J.; Fang, A.; Kolthammer, B. W. S.; Reed, D.; Thompson, J. L. *Inorg. Chem.*, in press, for an analysis of the electronic structure of $Cr(CO)_5NHC_5H_{10}$.

Table XIV. Activation Parameters for $M(CO)_5$(amine) and $M(CO)_5$(amine)·base Dissociative Processes in Hexane

complex	ΔH^*, kcal mol^{-1} [a]	ΔS^*, eu[a]
$Cr(CO)_5NHC_5H_{10}$ [b]	25.6	2.4
$Cr(CO)_5NHC_5H_{10}\cdot OP(n\text{-}C_4H_9)_3$ [c]	24.3 ± 0.6	1.6 ± 1.8
$Mo(CO)_5NHC_5H_{10}$ [d]	23.6 ± 1	5.4 ± 3
$Mo(CO)_5NHC_5H_{10}\cdot OP(n\text{-}C_4H_9)_3$ [c]	19.3 ± 3.1	−9.8 ± 10.3
$Mo(CO)_5NHC_5H_{10}\cdot THF$	23.0 ± 2.1	−1.9 ± 6.8

[a] Uncertainties are 95% confidence limits. [b] Uncertainties are not reported for this compound since the decomposition was measured at only two temperatures. [c] Approximate estimate from all maximum rates for substitution reactions in Tables VII and X. [d] Data taken from ref 1.

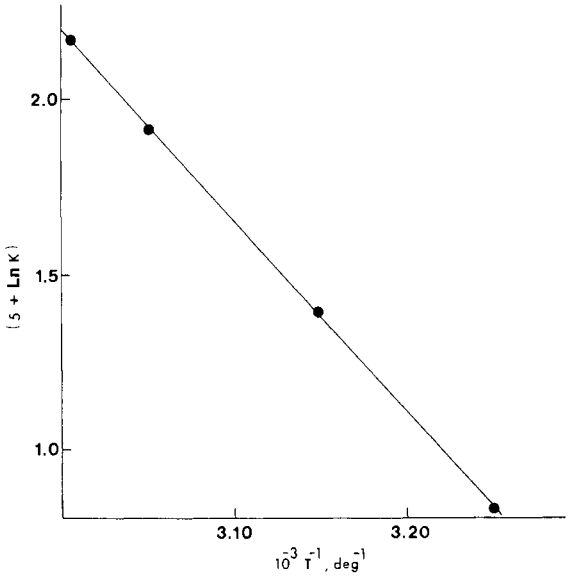

Figure 8. ln k as a function of T^{-1} (K) for the disappearance of the $Cr(CO)_5NHC_5H_{10}\cdot OP(n\text{-}C_4H_9)_3$ outer-sphere complex in hexane.

I_d and D mechanisms when changing solvents, where S is a solvent with an accessible lone pair (e.g., THF) and S′ is a π base (e.g., benzene). Solvents may thus act as catalysts or inhibitors in these substitution reactions through specific solvent effects.

The limiting rate in the dissociative interchange mechanism is not radically different from those observed in the D pathway. Both ΔH^*[4] and ΔS^*[40] have been implicated as making the major contribution to this small rate enhancement for I_d vs. D processes. Unfortunately, because of the uncertainties in the activation parameters determined in this investigation for these two processes, no definitive assessment of the origin of this rate enhancement in the I_d pathway is possible.

Concluding Remarks

The intermediacy of hydrogen-bonded species may be relevant to a large variety of amine substitutional processes, ranging from those involving coordination complexes to those of biological importance.[41] Since the rate of amine substitution is sufficiently slow when compared with the rate of formation of the hydrogen-bonded complex, it should be reiterated that the two incoming ligand-dependent reaction pathways described in skeletal form below are kinetically indistinguishable.[42] That is, the dissociative interchange indicated in process A, where the hydrogen-bonded species is

process A

$$M\text{-}NHR_2 + OPR_3 \overset{K_c}{\rightleftharpoons} M\text{-}NHR_2\cdot OPR_3$$

$$M\text{-}NHR_2\cdot OPR_3 \xrightarrow{k_c} M\text{-}OPR_3 + NHR_2$$

$$\text{rate} = k_cK_c[M\text{-}NHR_2][OPR_3]$$

process B

$$M\text{-}NHR_2 + OPR_3 \overset{K_c}{\rightleftharpoons} M\text{-}NHR_2\cdot OPR_3$$

$$M\text{-}NHR_2 + OPR_3 \xrightarrow{k_2} M\text{-}OPR_3 + NHR_2$$

$$\text{rate} = k_2[M\text{-}NHR_2][OPR_3]$$

an intermediate in the reaction, is kinetically indistinguishable from process B attack of the base at the metal or carbonyl carbon atom centers in which the hydrogen-bonded species does not lie along the lowest energy reaction path in going from reactants to the transition state. The criteria applied here, which conclude that a dissociative interchange type mechanism (A) is operative in the base-catalyzed amine substitution process, are the similarities between the activation parameters and metal dependence with those observed in dissociative processes.[4,30]

Acknowledgment. The partial financial support of this research by the National Science Foundation (Grant CHE 80-09233) is greatly appreciated.

Registry No. $Mo(CO)_5(C_5H_{10}NH)$, 19456-57-6; $Cr(CO)_5(C_5H_{10}NH)$, 15710-39-1; $W(CO)_5(C_5H_{10}NH)$, 31082-68-5; $Mo(CO)_5(C_6H_{11}NH_2)$, 21199-57-5; $Cr(CO)_5(C_6H_{11}NH_2)$, 15134-57-3; $Mo(CO)_5NH_3$, 13931-12-9; $P(C_6H_5)_3$, 603-35-0; $P(n\text{-}C_4H_9)_3$, 998-40-3; $OP(n\text{-}C_4H_9)_3$, 814-29-9; THF, 109-99-9; $OP(OCH_3)_3$, 512-56-1; py, 110-86-1; $(CH_3)_2CO$, 67-64-1; C_6H_6, 71-43-2; $(C_6H_5)_3PO$, 791-28-6; C_4H_8ONH, 110-91-8; NH_3, 7664-41-7; $C_5H_{10}NH$, 110-89-4; $(C_6H_5O)_3P$, 101-02-0; $(C_2H_5O)_3P$, 122-52-1; $(n\text{-}C_4H_9O)_3P$, 102-85-2; $(CH_3)_2C_6H_5P$, 672-66-2; $(C_6H_{11})_3PO$, 13689-19-5.

(40) Lalor, G. C. *J. Chem. Soc. A* **1966**, 1.

(41) Ewen, J. A.; Darensbourg, D. J. *J. Am. Chem. Soc.* **1976**, *98*, 4317.

(42) Halpern, J. *J. Chem. Educ.* **1968**, *45*, 372.